The practical optimisation of complex architectural forms

Zhenzhou Weng, Alfonso P. Ramallo-Gonzlez, David A. Coley

Department of Architecture and Civil Engineering, University of Bath, UK

27^{th} November 2014

Abstract

The energy consumption of a building and its internal conditions are intimately related to its shape. There have been various attempts to use computer-based optimisation within a thermal simulation environment to produce designs with minimal energy consumption. Most of these studies have looked at optimising parameters such as U-values and glazing ratios, but a small number have looked into the form of the building, but in a way that does not naturally fit with the human-led design process. In this paper, the first practical methodology for optimising complex building facades and internal layouts is presented. The method allows for a free exploration of new, non-preconceived, design solutions in a way that complements the natural design process. The method has been tested on a design with eight facades. The rapid convergence of glazing ratios for all runs indicates their significance in the energy performance of a building. The solutions display a high degree of variability of floor shape without a compromise in performance, which indicates that human judgment can still be used as a filter even within an optimising framework. Typical solutions produced by the method show an annual total energy demand of 56 kWh/m^2, 51% lower than typical for the region in which the building was sited.

Keywords

GA, building form, low-energy design, multi-zone, encoding floor plan, layout, constrained optimisation, geometry optimisation

The final publication is available at www.springerlink.com

1 Introduction

1.1 Optimisation in building design

There have been several attempts to use automatic optimisation within a thermal simulation environment to produce building designs with minimal energy consumption (Marks 1997; Peippo et al. 1999; Bouchlaghem 2000; Coley and Schukat 2002; Holst 2003; Zhou et al. 2003; Wetter and Wright 2004; Wetter 2005; Ramallo-Gonzlez and Coley 2014). However, such work tends to see optimisation as a way of finding the parameters of a given building that will make it best in terms of energy efficiency by solely looking at scalar parameters (for example U-values, windows areas etc.). Whereas examples in which optimisation is used for the production of the whole architectural form are scarce. Previous work (Coley 1999) showed that optimisation was useful in optimising the perimeter-to-floor-area-ratio; however this is a long way from the derivation of a complete form. Mark (1997) and Wang et al. (2006) both proposed methods to generate basic building forms based on a set of optimisation objectives. However the use of automated optimisation of building form via a process which is cognisant of the inevitable geometric constraints provided by the organisation of internal spaces has not been previously considered. These constraints are important, because the approximate floor area of internal spaces is decided before the exterior form. For example, classrooms normally have minimum and maximum sizes, and there are expectations about domestic room size, or cellular office size in various parts of the world.

The plan shape and layout of a building are for practical and aesthetic reasons often determined soon after completion of the conceptual design phase (AIA 2011). It is known however that alterations to the basic shape can affect energy performance by up to 40% (Wang et al. 2006). Thus it would seem sensible to apply optimisation during this phase, and not just later when considering parameters such as U-values, thermal mass and glazing ratio. Indeed, minimising energy use is just one example where this optimise-early-ratherthan-later philosophy is likely to be beneficial.

A confounding issue is that buildings are complex entitles, and the alteration of any parameter may reduce or increase energy consumption depending on the values of a group of other parameters. Hence optimisation cannot be done independently for each variable, with for example, the optimisation of glazed area, followed by the optimisation of the distribution of the windows within the facades (Tuhus-Dubrow and Krarti 2010). Optimisation needs to be done simultaneously on the whole design. Given the number of possible parameters, and the number of possible values for each parameter, simple estimation of all possible combinations is also not possible. There is therefore the need to use some form of automatic self-steering

optimisation algorithm that will explore potentially good solutions (Caldas and Norford 2002). In this work we have used a genetic algorithm for this purpose, as it has been used previously in (Holland 1975; Goldberg 1989; Mitchell 1998; Coley 1999) and because it can be used to explore large search spaces, and objective functions with multiple local optima, whereas traditional methods such as hill climbing might well get stuck in the local optima (Kohonen 1999).

1.2 Genetic algorithms (GAs) and the optimisation of form

GAs were introduced by Holland in 1975 (Holland 1975) to model evolution, but it was soon realised they could be used as general function optimisers; and after the publication of Goldbergs textbook (Goldberg 1989), they became popular tools for scientists and engineers.

GAs are population-based algorithms, meaning that in each iteration, not one but a group of points in the decision landscape are evaluated. The points evaluated are termed individuals, and these individuals represent a point in the decision space encapsulated by encoding the values of the decision variables as a string. Keeping with the evolutionary theme, the variables stored in the string are termed chromosomes.

The strings can be in the form of a list of real numbers, with one number representing each attribute, or they can be binary strings with a simple proportional mapping to the real or integer value of the decision variable, or discrete possibilities.

During optimisation, the current process undergoes: selection to be included in the next generation, based on their fitness as measured by the function being optimised; crossover, where pairs of candidates swap some chromosomes; mutation, where the value of one or more parameters within an individual is randomly altered. The termination of the algorithm normally occurs after a fixed number of generations or when the rate of change in improvement of the best solution has almost halted.

Kawakita (2008) concluded in his review that architectural design objectives are interrelated and have contradictions and their relative importance or necessity will vary case by case. Thus it would seem impossible to frame a universal machine-based optimisation without human judgment. He also claimed the indispensable need for architecture to rely on designer preferences to generate the original design characteristics. Our study appreciates the above concern and reflects it in its optimisation strategy.

Chouchoulas (2003) used a GA during conceptual design by generating space formation rules that were able to evolve a building stack comprised of modular blocks, while the desired space types (e.g. apartment, balcony), their proportions and spatial relationship between them still needed to be set by the user, which also suggests the necessity for humans to provide a rudimental form of design. Indeed, it is probably impossible to start a sensible optimisation, i.e. one that leads to a valued product, from a blank sheet of paper with only a list of requirements or criteria.

In our work the optimisation starts with the interaction of the designer with a graphical user interface written to extract the minimum amount of information needed about the approximate form of the building. This information forms the constrains. This builds on previous work (Wang et al. 2006) where a GA was applied to floor shape optimisation under the requirement to minimise the life-cycle environmental impact. The floor is treated as a polygon and the relative location of edges are encoded to represent the shape (giving a generalised shape description method); however, the varying of floor shape is not constrained by the rooms enclosed in it. As shown in Fig. 1, in such an approach if the plan layout is modified during the optimisation, the internal partitions will have to be modified in order to solve any spatial conflicts.

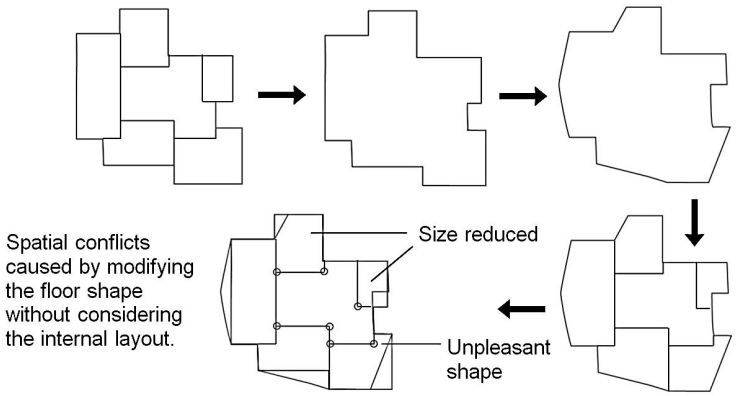

Fig. 1 Conflicts between floor reshaping and internal room distribution. These conflicts need to be resolved if impractical/unusable shapes are to be avoided and room areas preserved

Dividing the floor into multiple spaces allows the occupancy density, artificial lighting and other equipment to be correctly distributed throughout the building depending on the requirements of each space and its occupants. In previous works on form optimisation, details about the occupants have not been included (Kawakita 2008). This would seem unwise once we attempt to optimise for en-

ergy use or other environmental parameters such as thermal comfort. Occupation densities, schedules and user type will influence the heat balance within zones and will therefore lead to different optimal/preferred envelope/facade designs, and this effect was observed in this research. It is worth noting that the use of a multi-zone model is essential if naturally and conditioned spaces on the same floor are to be handled correctly.

2 Previous work

The term, rules of design, refers to the principles by which designers can expect certain performance levels or the values of set objective functions to be achieved. For instance, guidelines in regulations are design rules, as they are general descriptions of the relationship between parameters. GAs can be applied to a population of different parameter sets and used to determine their fitness by reviewing the overall performance of designs generated by them and thereby find robust design principles. The idea of optimising the path to solutions rather than the solutions directly can be traced back to early applications of GAs on automatically written computer programs (Mitchell 1998). Similarly, in architecture, following certain rules (e.g. not locating bedrooms facing a busy street) are used when exploring design alternatives by hand. This manual form-finding process is always limited by time, personal style and imagination, and hence augmenting human design with computers with pre-set rules can be seen as expansive rather than restrictive, and has been presented as such by architectural researchers (Coley and Winters 1997; Kolarevic 2000).

Watanabe (2000) described the partition and connection of spaces in architecture as a web frame, which enabled computers to understand human preferences and considerations as the behaviour of the frame. Through interaction between the user and the web frame, repetitive and recognizable configurations of the web frame are learnt by the computer as a set of rules to regulate the form finding. Further form finding is then undertaken solely by the computer. Although this method can be used as a way of using artificial intelligence to systematically generate pleasant designs, it does not allow evaluation of designs by aspects such as in-building pedestrian flow, or energy use.

Other research on spatial relationship generation has used the concept of shape grammar, introduced by Stiny and Gips (1972), which perceives individual spaces as elemental building blocks and the transformation and combination of them as a sequence of actions taken to form the final design. The whole process could thus be modulised and coupled with a GA to find desirable rules (e.g. if the living room

and the kitchen are on the north, position a bedroom on the east). Elezkurtaj and Franck (2001) proposed the use of a GA to minimise the overlap and gap between rooms with different functions within a given area, with the floor plan generated by shape grammar rules. Chouchoulas (2003) extended the application to three-dimensional building blocks.

Due to the development of panelisation technology, architecture with no clear boundary between the vertical and horizontal surfaces can now be undertaken (Kolarevic 2000). Unlike conventional buildings (which can be represented by floor plans and heights), their facades have non-linear variations and require a full three-dimensional description. The potential form of such buildings, and any structural issues are now being studied using GAs. For example Chronis et al. (2011) attempted to optimise a nonuniform rational B-spline (NURBS) surface on the overall wind load through evaluation by using Fast Fluid Dynamics.

Turrin et al. (2011) coupled a GA with finite element analysis to optimise the tessellation-cladding configuration of a NURBS surface and another surface described by a mathematical function of the mechanical load. Apart from structural performance, the solar gains and natural light within the building were evaluated: the objective being to maximise the daylight factor and control solar gains. The surface was encoded as a grid of points for finite element analysis but with a separate finished cladding system generated for the analysis of the solar gains.

Minimising energy consumption from heating, cooling and artificial lighting, within such cellular fenestration designs was discussed by Wright and Mourshed (2009). Several reference points were set in the room to enable daylight compensation, which as they concluded, results in more glazing cells on the top area of wall. An optimal range of glazing ratio can be observed, while there is no apparent correlation between energy use and the pattern of glazing cells. Caldas and Norford (2002) attempted to find an optimal glazing ratio with a single window on each wall and found the glazing ratio on each wall stayed within a fixed range (but different for different orientations) when they repeated the optimisation runs. GAs have been used on the optimisation of real architectural projects, for example the Light House by Gianni Botsford Architects (2005). Here the GA was used to optimise the location of opaque, translucent and transparent glazed elements on the roof to optimise daylight factor and direct glare. In separate work, Kawakita (2008) explored the possibility of achieving specific daylight level at a set of reference points with cellular glazed facades.

GAs developed for optimising building designs normally use encoding methods that follow the design process.Designers often work first using a bubble diagram and then complete the outline to enclose the space. This convention can be seen

in many applications of GAs, including the work by Rosenman and Gero (1999); however energy simulation requires explicit descriptions of the thermal boundaries, which is why studies focusing on energy performance choose to encode the building perimeter instead of following the spatial-element-based approach. Some such studies have assumed the building is a rectangle or other basic geometry (e.g. an L-shape) and only varied the aspect ratio. Tuhus-Dubrow and Krarti (2010) used seven shape options to represent typical residential buildings. However in general pre-fixing the shape is design limiting, and a more general approach to shape optimisation is desired, and is addressed in the work reported in this paper.

2.1 Encoding of forms using GAs

This section discusses the ways in which a building form can be encoded in a GA, assuming the information needed for completing the building form is the shape of its floor plan and the floor-to-ceiling height is predefined. Twodimensional shapes are comprised of a series of edges and the nodes joining them, which means using these elemental components as chromosomes within a GA will not limit the complexity of the shape that can be encoded. Wang et al. (2006) discussed several edge-based encoding methods. The two main types are the length-angle method and the length-bearing method. The length-angle method describes the floor plan from a starting point (P1) and defines each edge by its length and the angle of rotation from the previous edge. Whereas in the length-bearing method, instead of using the rotation angle between edges, the angle (bearing) between each edge and the true north (counter clockwise) is used. These two methods can be seen in Fig. 2.

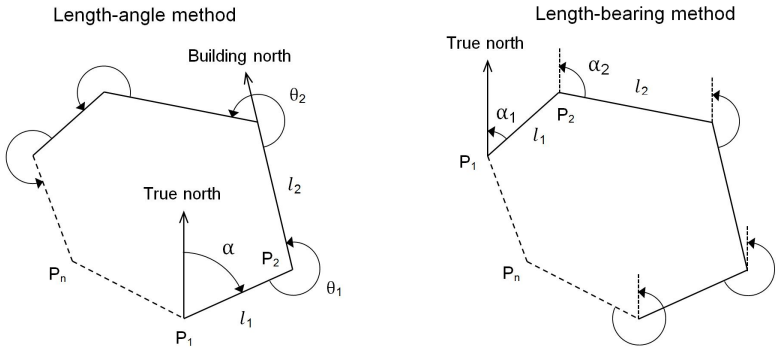

Fig. 2 Length-angle and length-bearing methods adapted from Wang et al. (2006)

Compared to the length-angle and the node coordinate method this length-bearing method is known to suffer the least from isomorphism or epistasis. As shown in

Fig. 3, if one wanted to encode the absolute coordinates measured from the global origin, it is possible that two different genes (coordinates) share an identical floor description, which can cause isomorphism, namely a phenotype (geometry) is not represented by one unique genotype (string); this not only makes the schema theorem (Goldberg 1989) which lies behind GAs invalid, but also uses extra time for unnecessary simulation. (In a GA the whole string of decision variables of one individual solution is termed its genotype, and what the string represents in the evaluation model for the optimisation is termed its phenotype).

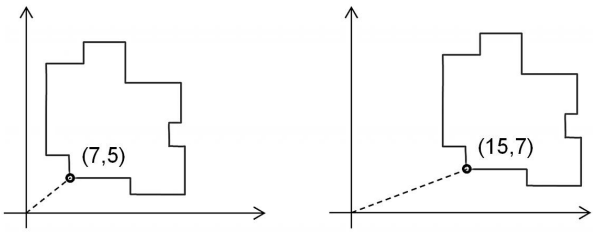

Fig. 3 Isomorphism problem in encoding absolute node coordinates

Length-angle and length-bearing both create epistasis. Epistasis refers to the conditions where the same genotype on a section of chromosomes could lead to different phenotypes depending on the value taken by other chromosomes on the string. Hence when the parameters of an upstream node are modified, the modification also affects the downstream nodes, as seen in Fig. 4.

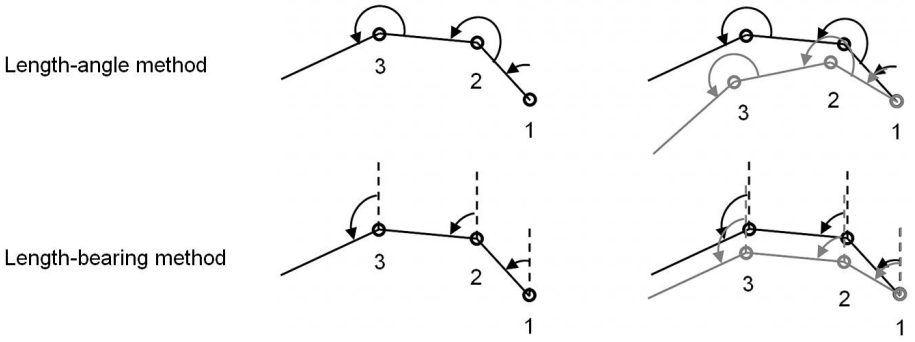

Fig. 4 Epistasis in the length-angle and length-bearing methods

It can be seen in Fig. 4 that while the genes of nodes 2 and 3 remain unchanged when modifying the angle or bearing of node 1, the locations of nodes 2 and 3 are forced to change, and if the parameters of node 2 are also modified, the influences will be accumulated at node 3. The effect is less significant with length-bearing because the angle is measured from an absolute direction and is thus independent

of the previous arms. Magnitude and angle represent a vector, and therefore the epistasis results from the potential to define a node with the same vector but a starting point sequentially varied by crossover and mutation. Hence identifying each node by a vector pointed from a fixed reference node (i.e. a relative origin) can reduce epistasis: the edge between nodes is still altered, but the change will not be accumulated, as shown in Fig. 5.

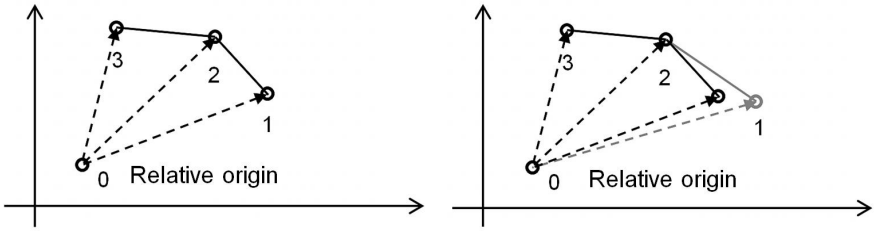

Fig. 5 Defining the location of nodes between edges with a relative origin

In the work by Wang et al. (2006), a pentagon floor plan was used as the basis of an edge-based encoding method, and a large combination of parameters, with low energy use or life-cycle cost, could be found. However constraints from the internal spatial-elements caused issues (see Section 1.2) and led to the method being inconsistent with the design process. In addition the approach was not multi-zone which is critical if the thermal performance of large buildings that could have both naturally ventilated and conditioned spaces is to be assessed. In our research an external node categorisation method, which not only encodes the location of the external nodes but also their connection condition with internal nodes, coupled with an area compensation scheme is developed, which can be applied to multi-zone buildings.

3 Methodology

A suite of software was created to apply GA-based optimisation to the shape selection of complete floors of small or large buildings. This involved the production of a bespoke encoding for the shape of a floor and the production of a series of new GA operators. As a proof of concept it was decided to apply the method to the problem of the minimisation of annual operational energy demand, although various other problems could have been studied, for example overheating or daylight levels. It would have been possible to link the GA with a simple energy model suitable for early stage design, for example a degree-days model; however it was decided to link it instead to EnergyPlus (Crawley et al. 2001). This had

the benefit of creating a powerful tool capable of not only early-stage analysis, but detailed analysis at any stage of a project. It also means the tool is easy to use by anyone with knowledge of EnergyPlus. It can thus be seen as a practicable optimisation tool, for use not only by building scientists, but also by the wider engineering community.

The main evolution program and file processing program are run in parallel and the flow chart of the system is presented in Fig. 6.

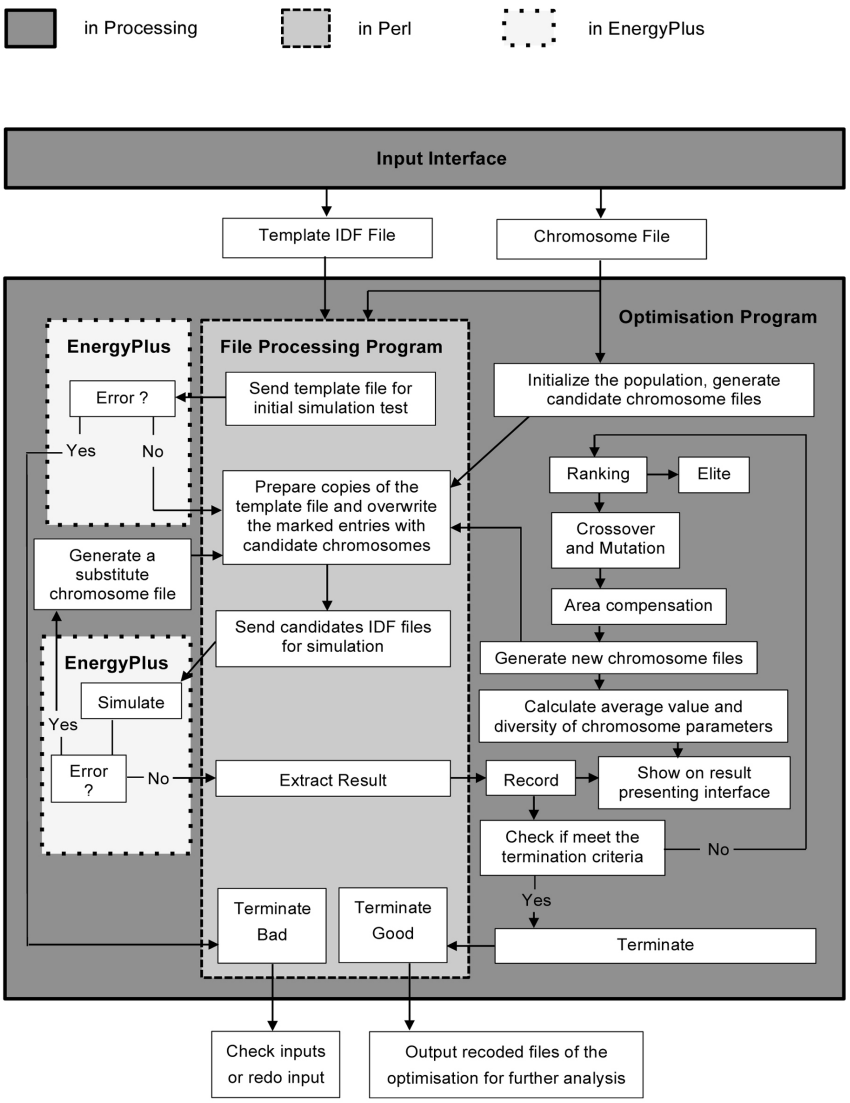

Fig. 6 Optimisation flow chart

The GUI was created using the Processing computer language (Fry and Reas 2012). This was linked to EnergyPlus via the exchange of text files.

Although many interfaces have already been developed for EnergyPlus (e.g. DesignBuilder, OpenStudio), a new GUI was required for this work. The GUI and EnergyPlus were linked together via a short program written in Perl, to help construct simulation files of the candidates and initiate simulation runs by EnergyPlus.

3.1 Building model

Figure 7 presents the general description of any design within the evolutionary program.

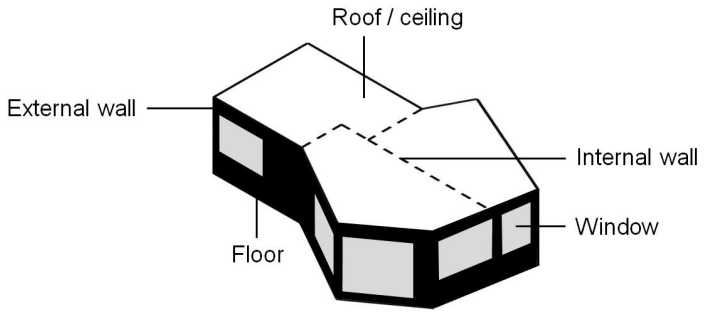

Fig. 7 General description of a design within the evolution program

Geometrically, all designs are prismatic and single-storey (multi-storey building can be created by stacking floors on top of each other). The shape is defined by the chromosomes at any point in the optimisation and the floor-to-ceiling height is fixed (initially specified by the user). The user can divide the floor into multiple zones (separated by internal walls) and different operating conditions (i.e. occupancy, ventilation) can be set for individual zones. Adjacency conditions of the floor and roof / ceiling depend on the floor type (i.e. ground, intermediate or top) as defined by the user. Encoding of the geometry will be discussed in Section 3.3, below.

Tables 1-3 show the fixed parameters used to complete the thermal description of the building in the case study. These comprise those not adjusted by the GA, and those variables under the influence of the GA over the range indicated.

The window used in the model is double glazed with low-e coating on the front panel and has a U-value of 1.8 W/(m^{2}K), a solar transmittance of 0.5 and a visible transmittance of 0.75.

Table 1 Constructions used for the building envelope (abbreviations refer to specific materials listed in Table 2)

Constructions					
Name	Roof	Ground floor	Intermediate floor	External wall	Internal wall
Layers of material	RG01 BR01 IN46 WD01	FLOOR-1	CC03	WD01 PW03 IN02 GP01	GP02 AL21 GP02

Table 2 Properties of materials used in the constructions of the building envelope in the case study

Properties of materials								
Name	Roughness	Thickness (mm)	Conductivity (W/(mK))	Density (kg/m^3)	Specific heat (J/(kgK))	Thermal emissivity	Solar absorptance	Visible absorptance
RG01	Rough	13	1.442	88	1674	0.90	0.65	0.65
BR01	Very rough	10	0.162	1121	1464	0.90	0.70	0.70
IN46	Very rough	87	0.023	24	1590	0.90	0.50	0.50
WD01	Medium smooth	19	0.115	513	1381	0.90	0.78	0.78
CC03	Medium rough	102	1.310	2243	837	0.90	0.65	0.65
PW03	Medium smooth	13	0.115	545	1213	0.90	0.78	0.78
IN02	Rough	108	0.043	10	837	0.90	0.75	0.75
GP01	Medium smooth	13	0.160	801	837	0.90	0.75	0.75
GP02	Medium rough	16	0.160	801	837	0.90	0.75	0.75
FLOOR-1	Rough	N/A	Thermal resistance 4.65(m^2.K)/W			0.65	0.65	0.65
AL21	N/A	N/A	Thermal resistance 4.65(m^2.K)/W			N/A	N/A	N/A

Table 3 Specifications of the HVAC system

Supply air temperature				Supply air moisture content	
Heating		Cooling		Heating	Cooling
50^{o}C		13^{o}C		0.015 g/g	0.01 g/g
Thermostat set-points					
Natural ventilation		Mechanical ventilation		Set-back (unoccupied period)	
Heating	Cooling	Heating	Cooling	Heating	Cooling
17^{o}C	25^{o}C	18^{o}C	23^{o}C	12^{o}C	30^{o}C

The heating and cooling systems are idealised systems with infinite heating and cooling power. Although we are aware of the limitations of this way of modelling, this option was selected as it facilitates the implementation despite the differences in geometry and characteristics of each solution.

To enable evaluation of naturally ventilated designs/zones, the airflow network model of EnergyPlus was applied (see EnergyPlus Input Output Reference P910 GroupAirflow Network (LBNL 2010)). The model considers both wind and buoyancy driven flow, and is capable of handling flow organisation with multiple openings, which allows it to distinguish between single-sided and cross ventilation. The ability to deal with natural and mechanical ventilation on the same floor of a building is one of the major objectives of the research. The automated wind pressure coefficients of EnergyPlus were applied for this study.

Various types of shading can be defined in EnergyPlus, including detached and attached objects. As detailed shading design is not expected in the conceptual phase, it is probably unnecessary to apply a complete set of shading devices, which will both considerably complicate the shading calculation and make it more difficult to understand the evolution results. Therefore only shading from a horizontal overhang has been includedhowever this could be expanded to cover all forms of shading.

Apart from heating and cooling, the total energy loads calculated for each design also include electricity for artificial lighting, the latter being dimmed in relation to the amount of daylight introduced via the windows. Reference points for dimming control are specified by the user through the GUI.

3.2 The graphical user interface

Central to the tool is the graphical user interface (GUI). This is comprised of a graphic plan layout input grid and other slides and textboxes, which are based on the controlP5 library (Schlegel 2012).

Table 4 summarises the available non-graphical inputs.

The graphic plan layout input grid covers all inputs relevant to building geometry. Only a single floor is optimised at a time, allowing for complex overall building shapes. The user can also declare the adjacency of the floor and ceiling/roof, and allocate windows and set them operable for natural ventilation.

The input of the initial plan layout and window/ventilation settings should follow the process below (Fig. 8).

Table 4 Non-graphic inputs in the GUI

Basic info and simulation control settings	Zonal occupancy conditions
Relative north axis	Occupancy schedules for weekday and weekend
Simulation period	Occupancy density
Local terrain (i.e. roughness of the local context, wind exposed condition)	Activity level
Shading calculation method (e.g. full exterior only or full exterior and interior)	Artificial lighting heat gain
Simulation time step	Electric equipment heat gain
Load and temperature convergence tolerance	Illuminance set-point for dimming control

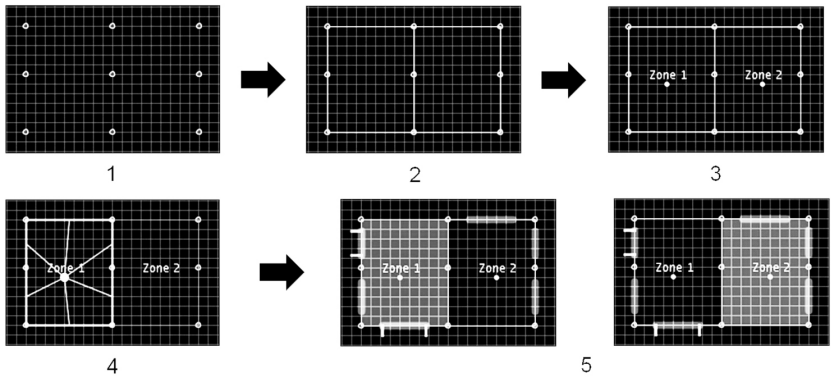

Fig. 8 Steps in inputting the initial plan layout and window/ventilation settings of the design

In step one, all nodes needed to define an external or internal wall need to be positioned. In step two, the nodes are linked to form the walls. In step three, zone points need to be allocated in each space enclosed by the walls, and in step four the walls need to be assigned to their associated zone points. Because the zone points also act as the reference points used in the daylight compensation calculation for dimming control, it is allowed and recommended to put multiple zone points in one zone for large or non-convex rooms where daylight level within the space is likely to be non-uniform. In step five the user can put windows (indicated as translucent grey stripes) on the walls and set them as operable (indicated as two white stripes extending from the window). The zone will be highlighted in light grey if it is naturally ventilated, otherwise mechanical ventilation is assumed.

A template IDF file and chromosome file are then automatically created to allow the main evolution program to initialise the evolution.

3.3 Encoding of building geometry

3.3.1 Outline

The encoding scheme used to describe the floor plan is shown in Fig. 9. A node-based description is applied. The internal nodes are fixed, while the external nodes are moved by GA operators during the evolution, i.e. internal walls between internal nodes are fixed but those between one internal and one external node vary (divisions that must not be modified (e.g. structural walls/points) can be fixed). One internal node is set as the relative origin as described in Section 2, and the location of all other nodes is defined as a the vector from this origin.

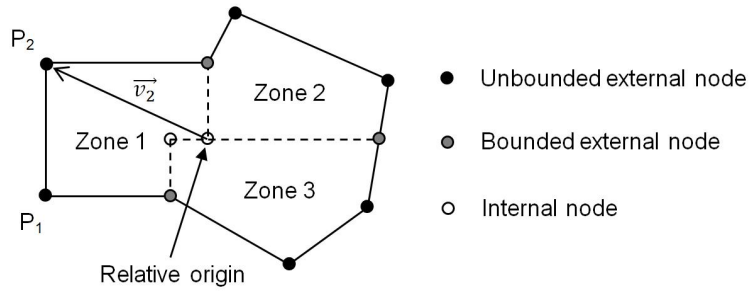

Fig. 9 Floor plan encoding

As previously stated, if the area of each zone could be maintained constant throughout the evolution and the occurrence of unrealistic shapes in buildings layout can be controlled, then the internal partitions will not have to be relocated to fix the conflicts, instead they become free to be modified under other design concerns. This requires the external walls to self-compensate for the change in area produced by the GA operations during the evolution. The area compensation scheme used to achieve this is inspired by the Partially Matched Crossover scheme proposed by Goldberg (1989).

To allow implementation of the scheme, the external nodes are further categorised depending on their boundary condition: bounded if connected to any internal node and unbounded if only connected to external nodes.

The scheme proceeds by first noting any change of area in each zone from the parent candidates caused by the GA operators. Then the nodes belonging to the zone are relocated, with the rest of the nodes used to compensate for this area change. This produces the child candidate, which bounds the same floor area. As can be seen in Fig. 10, modifying one bounded node reshapes the two zones sharing the node, hence it would be more difficult to use them for compensation

to satisfy both zones and therefore it is better to apply crossover and mutation on them first. The second principle is that when one node is being moved (either by the GA operators or the area compensation scheme), the two adjacent nodes will be fixed to ensure Eq. (1) is valid.

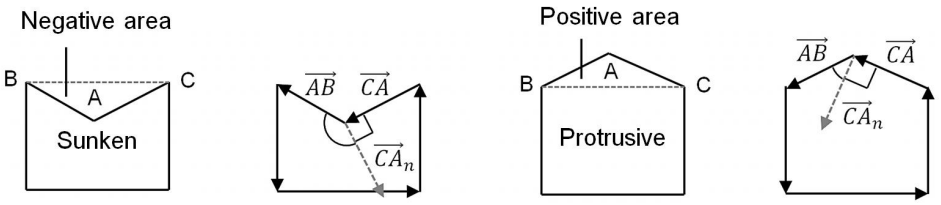

Fig. 10 Vector-based area calculation method to eliminate any concave-convex ambiguity

For a triangle ABC formed by one node being moved and its two adjacent nodes, its area can be calculated from the coordinates of the nodes using:

$$\begin{aligned} S_{ABC} =& |\overrightarrow{AB} \times \overrightarrow{AC}|/2 = |(X_B - X_A)(Y_A - Y_C) \\ & - (X_A - X_C)(Y_B - Y_A)|/2 \end{aligned} \tag{1}$$

where S_{ABC} is the surface area of triangle ABC, $\overrightarrow{AB}$ the vector from point A to B (with the same convention by applied to the other vectors) and X_B the X coordinate of point B (again with the same convention applying to the other coordinates).

This only gives the absolute value. As the triangle is not always protrusive (relative to the zone), the software needs to detect whether the area is positive or negative. The floor surface is defined as a counter clockwise vertex, as required by EnergyPlus, and this can be harnessed, as shown in Fig. 10, to eliminate the concave-convex ambiguity.

The dashed arrow indicates the counter clockwise rotated normal vector of $\overrightarrow{CA}$, denoted as $\overrightarrow{CA_n}$, which forms an obtuse angle with $\overrightarrow{AB}$ when the triangle is sunken, and an acute angle when the triangle is protrusive, thus the point product of $\overrightarrow{AB}$ and $\overrightarrow{CA_n}$ will be negative in the former and positive in the latter, and the following derivation:

$$
\begin{aligned}
&((X_B - X_A)(Y_A - Y_C) - (X_A - X_C)(X_B - Y_A))/2 \\
=&(X_B - X_A, Y_B - Y_A) \cdot (Y_A - Y_C, X_C - X_A)/2 \\
=&\overrightarrow{AB} \cdot \overrightarrow{CA_n}/2
\end{aligned} \tag{2}
$$

It shows that the magnitude of the dot product is equal to the area of the triangle. Hence $\overrightarrow{AB} \cdot \overrightarrow{CA_n}/2$ is concaveconvex sensitive and will be used to calculate the area change caused by moving point A.

For point A' (i.e. altered point A), the area change ΔS will be

$$
\begin{aligned}
\Delta S =&((X_B - X_{A'})(Y_{A'} - Y_C) - (X_{A'} - X_C)(Y_B - Y_{A'}))/2 \\
&- ((X_B - X_A)(Y_A - Y_C) - (X_A - X_C)(Y_B - Y_A))/2
\end{aligned} \tag{3}
$$

where $X_{A'}$ is the X coordinate of point A' (the same convention being applied to the other coordinates).

The process of relocating the unbounded node adjacent to point A' (e.g. point B) to compensate for the area change caused by moving point A is as follows.

Fig. 11(a) shows the area change (in grey) that results from moving point A, and Fig. 11(b) shows the room plan after this movement. Point B will then be relocated to return the size of the room back to its original value, while as shown in Fig. 11(c), the new location of point B could be anywhere on line b, which is parallel to line $A'D$, if no extra rule is applied. To avoid unrealistic room plans the new location of B is kept relatively close to its old location.

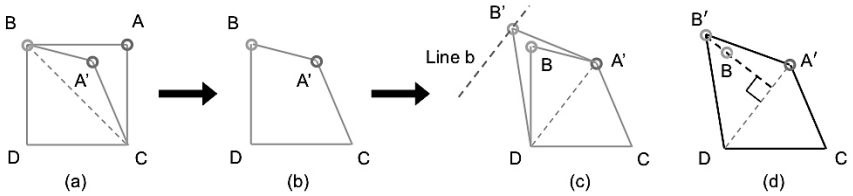

Fig. 11 Determination of the new location of unbounded nodes

Thus only the height of the triangle $A'BD$ will be varied. For point B' being relocated from point B for area compensation, BB' is perpendicular to the base

of triangle *A'B'D* (*A'D*), as shown in Fig. 11(d). The coordinates of *B'* can then be obtained with:

$$((X_D - X_{B'})(Y_{B'} - Y_{A'}) - (X_{B'} - X_{A'})(Y_D - Y_{B'}))/2 - ((X_D - X_B)$$
$$(Y_B - Y_{A'}) - (X_B - X_{A'}) - (X_B - X_{A'})(Y_D - Y_B))/2 = \Delta S \quad (4)$$

$$(X_{B'} - X_B)(X_D - X_{A'}) + (Y_{B'} - Y_B)(Y_D - Y_{A'}) = 0 \quad (5)$$

If a zone has only one unbounded node, it will skip the GA operators and the new coordinates will be derived from area compensation. If more unbounded nodes exist, half will be obtained via crossover and mutation and the rest will be determined by compensation following the rules defined in Section 3.4.

3.3.2 Windows

Each window is described by four parameters: the coordinates of the starting point (x, y), relative to the lower-left corner of the wall, and the width and height. Therefore direct exchange of window parameters via the GA operators does not ensure the sensible inheritance of the glazing configuration on each wall and the window may exceed the wall boundary and cause a simulation error. To overcome this, the proportional location and size of the window in the parent candidate is calculated, and multiplied by the wall length of the child candidate to obtain the absolute values of the window parameters, i.e. the window is resized according to the dimensions of the new wall on which it is fitted, but the glazing-to-facade ratio/configuration is maintained, as shown in Fig. 12.

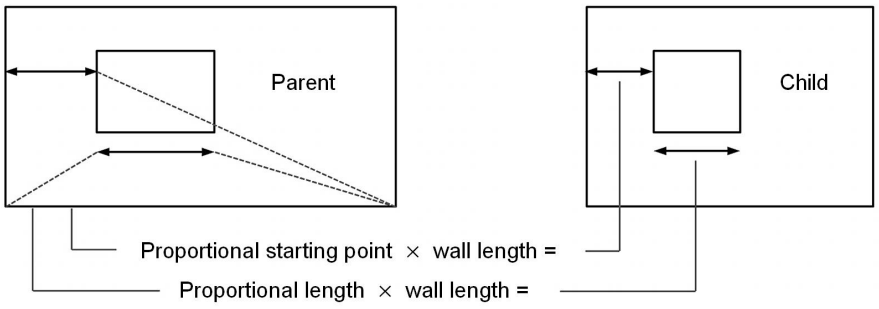

Fig. 12 Exchange of proportional window parameters

Any shading overhang has the same width as the window to which it is attached, and its depth has a value between 0 and 50 cm initially chosen randomly by the

program. In the results presented here, random values between 22^{o}C and 24^{o}C were assigned as window opening set-points (indoor air temperatures) for each candidateone setting per monthalthough other algorithms for opening the windows could easily be used.

3.4 Selection, crossover, mutation and termination

The population size was set to 30 individuals. Individuals were ranked according to their energy use (heating, cooling, artificial lighting), and then selected to mate with each other dependent on their rank. The top-two best performing candidates are considered as elite individuals (Coley 1999) and they pass directly to the next generationthereby ensuring the best designs cannot be eliminated between generations. The other 28 child candidates for the next generation undergo mutation and crossover. (Crossover is the exchange of chromosomes between two candidates. To perform crossover the individuals are selected and between a pair of individuals, one or more chromosomes of one individual are assigned to another individual at the same location on the string.)

This study applied a parameterised uniform crossover as follows. For each chromosome of a selected candidate, there is a fixed probability that it will be exchanged with the same chromosome from the individual it is mating with. The probability of exchanging chromosomes is set at 0.5 in this study. Within the group of the selected individuals, the probability of two being picked for crossover decreases linearly with rank.

Mutation is an additional random manipulation of the chromosomes of the selected individuals. For the design being evolved by the program, the settings shown in Table 5 were applied. Different values can be used for other designs and appropriate values can be estimated through running several evolutions with different mutation settings.

Table 5 Mutation settings applied on the design being evolved and discussed in Section 4

Probability of mutation for each chromosome	External node	Window	Shading	Ventilation set-point (indoor air temperature)
15%	Within a square bounding box with 1.0 m side length centred at the original location	Within 10% on all the proportional parameters	Within ±5 cm with lower limit at 5 mm to represent no shading	Within ±1^{o}C

The process of applying crossover and mutation for external nodes with area compensation is shown in Fig. 13.

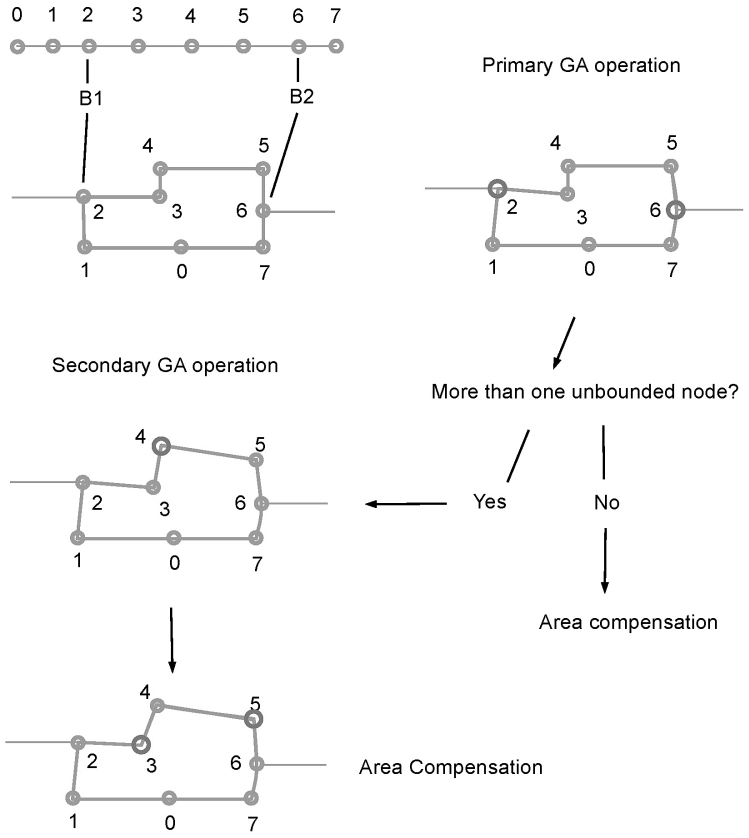

Fig. 13 Process of applying GA operators on external node parameters with area compensation

When more than one unbounded node is present between the two bounded nodes (B_1 and B_2), as shown in Fig. 13, after the bounded nodes are moved (the primary GA operation), half of the unbounded nodes will also be moved by the GA operators (the secondary GA operation) and the remaining half will be used to compensate for the area change caused by the crossover and mutation.

Therefore rules need to be defined to identify which half of the unbounded nodes will undergo crossover and mutation. According to the principle introduced in Section 3.3, when any node is moved, the nodes adjacent to it need to be fixed to make the calculation described in Section 3.3 valid; hence no two conterminous nodes should be selected for the secondary GA operation. Thus the following rules emerge. When one node presents between the bounded nodes, it will be relocated to allow area compensation directly. When there is an even number of unbounded

nodes, the one next to the bounded node 1 (B_1) and any node two nodes away from that node will be moved by the GA operators. When there are an odd number of unbounded nodes, the node two nodes away from the bounded node 1 (B_1) and any node two nodes away from that node will be moved by the GA operators. Figure 14 shows the rules graphically.

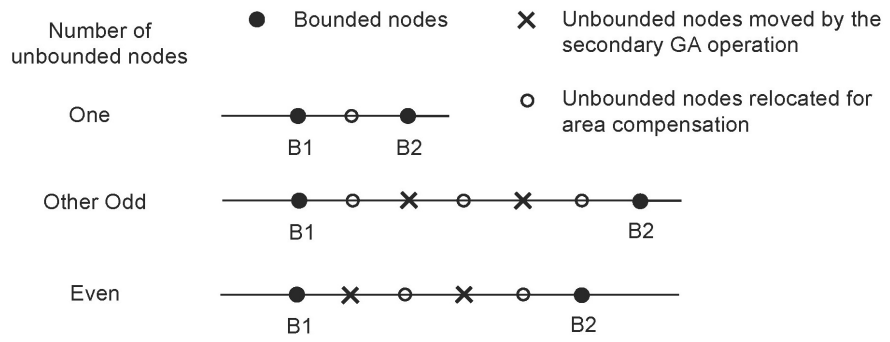

Fig. 14 Rules for selecting the unbounded nodes for the secondary GA operation

The maximum number of generations is set to 100. However, to save processing time, termination is triggered if the change in energy consumption of the best individual remains below 0.1% for more than 10 generations.

4 Application and results

In order to study the capabilities of the method, the tool was used to optimise the shape of a 240 m^2 single-floor building with 8 facades and 2 zones (the tool can optimise a floor of a maximum 20 facets and 12 zones). The weather file used is from Hangzhou (39.23^o N, 120.17^o E) (U.S. Department of Energy 2012). Hangzhou is located in the Hot Summer Cold Winter (HSCW) climate zone in China, which has distinct seasons. Simulations were first carried out in January (winter), April (representing both spring and autumn) and August (summer), as this represents all local seasons but reduces run times. Unlike in most simulation work, these seasons have been kept separate and with the optimisation running independently for each season. This is because we want to explicitly study how optimal form is related to each season, i.e. is the optimal form likely to be the optimal form in another season. The results were then explored, in part to see if

the results were consistent with the instinctive, qualitative analysis a good design team might bring to a project, but also to see if the system is capable of adjusting the form in a rational way.

The building was assumed occupied from 07:00 to 19:00 during weekdays and 09:00-17:00 during weekends. Occupancy densities of 0.1 to 0.4 person/m^2 were used and various ventilation strategies applied (including cross ventilation (CV) and mechanical ventilation (MV) with a constant flow of 10 L/(sperson)). An optimisation using a full-year of simulation was also performed to test the methodology on its ability to produce design solution with the lowest overall annual energy consumption. The runs were performed in a laptop with an Intel Core i5 2.53 GHz CPU and memory of 1 GB 1067 MHz DDR3. Each run took around 3.5 hours to complete (the full-year run took around 30 hours).

4.1 Evolution of the decision variables

An interface to help visualise the buildings produced and their performance was created. The population average (E_{ave}, black spots) and lowest energy consumption (E_{min}, grey spots) of any individual in the population are plotted for a run in Fig. 15.

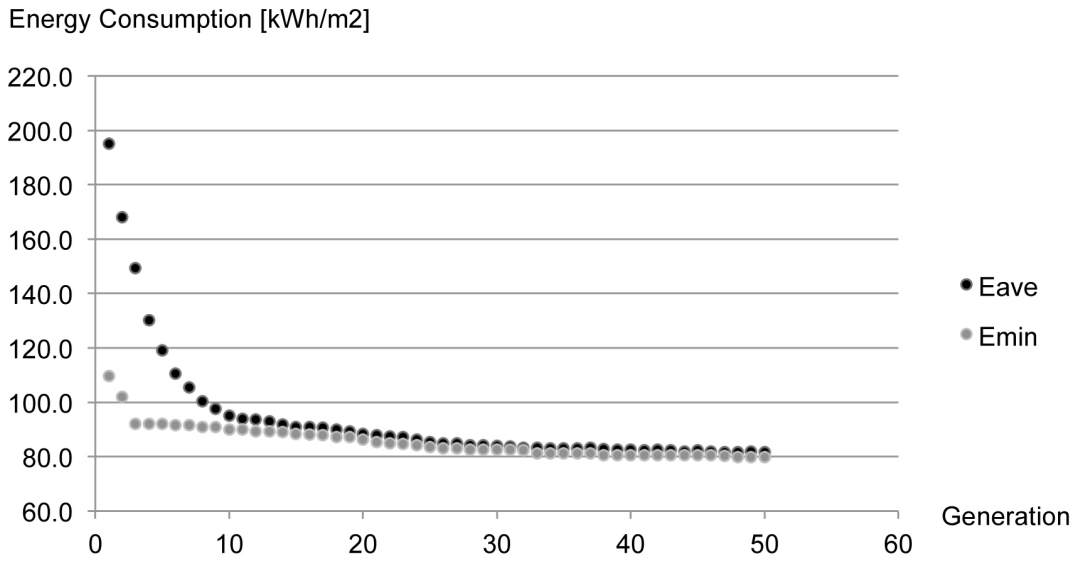

Fig. 15 The population average (E_{ave}) and lowest (E_{min}) energy consumption of an example run

Each scenario was run five times. The largest difference in E_{min} achieved at termination among all runs for any scenario was 0.1%, indicating that all runs of a single scenario approach the same optimum.

Window areas and glazing ratios converge quickly after 10 to 15 generations in all runs (Fig. 16), which demonstrates their significant influence on energy performance, as the schema theorem implies that genotype selection will first occur on the loci with more distinctive discrepancy in their phenotype to eliminate the lower-order schema with low average fitness.

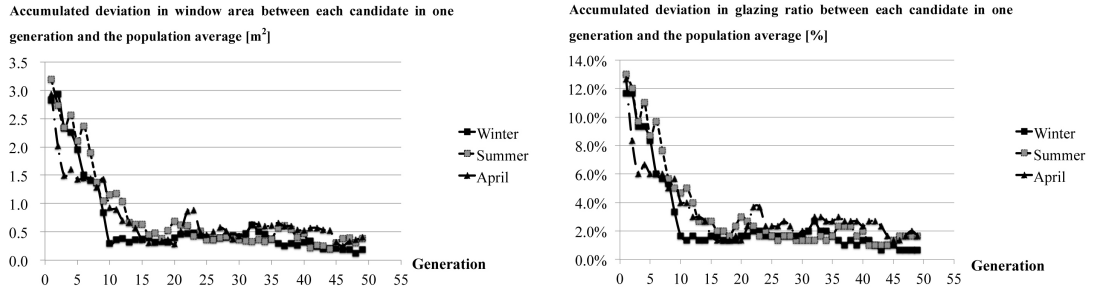

Fig. 16 Window area and glazing ratio are seen to converge rapidly in the seasonal runs

Shading depth, wall length and orientation do not seem to converge in a simple way (Fig. 17).

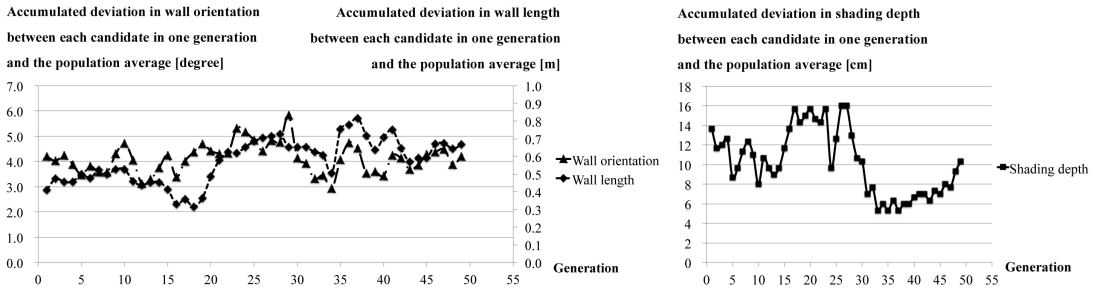

Fig. 17 Shading depth, wall length and orientation show no simple convergence

Variation in the ventilation set-point (Fig. 18) clearly demonstrates the impact ventilation has on the buildings overall performance. For example the set-point fails to converge in the summer runs, presumably because the hot outdoor air can rarely be used for cooling, whereas in April natural ventilation is frequently used by the occupants and hence convergence occurs.

The average vertical distance from the wall origin settled at around 1.1 m to 1.5 m for all windows, showing the preference for the system to locate the window in

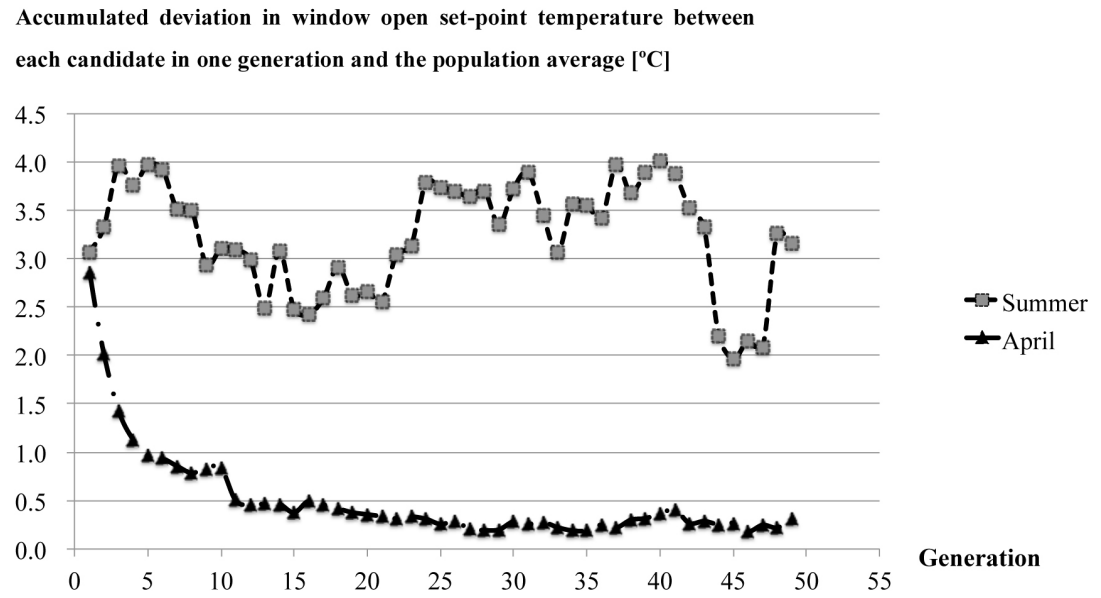

Fig. 18 Ventilation set-point convergence

the top half of the wall. This is consistent with results presented in the study by Wright and Mourshed (2009) and would seem reasonable as this would allow more daylight to reach the central area of the internal space behind the window.

4.2 Seasonal scenarios

The forms of the optimised designs of the winter, summer and April scenarios are described and analysed in this section. In all cases occupancy was set to 0.1 person/m^2.

As shown in Fig. 19, the glazing ratios on the north facades are much smaller in the winter results compared to the other two seasons. The sizes of south, east and west windows are similar between summer and winter designs, while those for April are considerably larger. Shading depth exceeds the maximum at initialisation on five of the walls in the summer design. By contrast, shading on the south facades of the winter design drops to 2 cm and is also lower on the other walls. Again, as expected, the south facing windows are found to be larger in the summer than winter, because in winter the system is attempting to improve the overall U-values of the facades. It would appear that although this leads to greater use of artificial light the efficiency of the lighting system is high enough to offset this. In summer, the increased cooling load that might be expected from large windows is partially

mitigated by the large overhangs that the summer runs create. The ventilation set-point converged to around 22.5^{o}C in April.

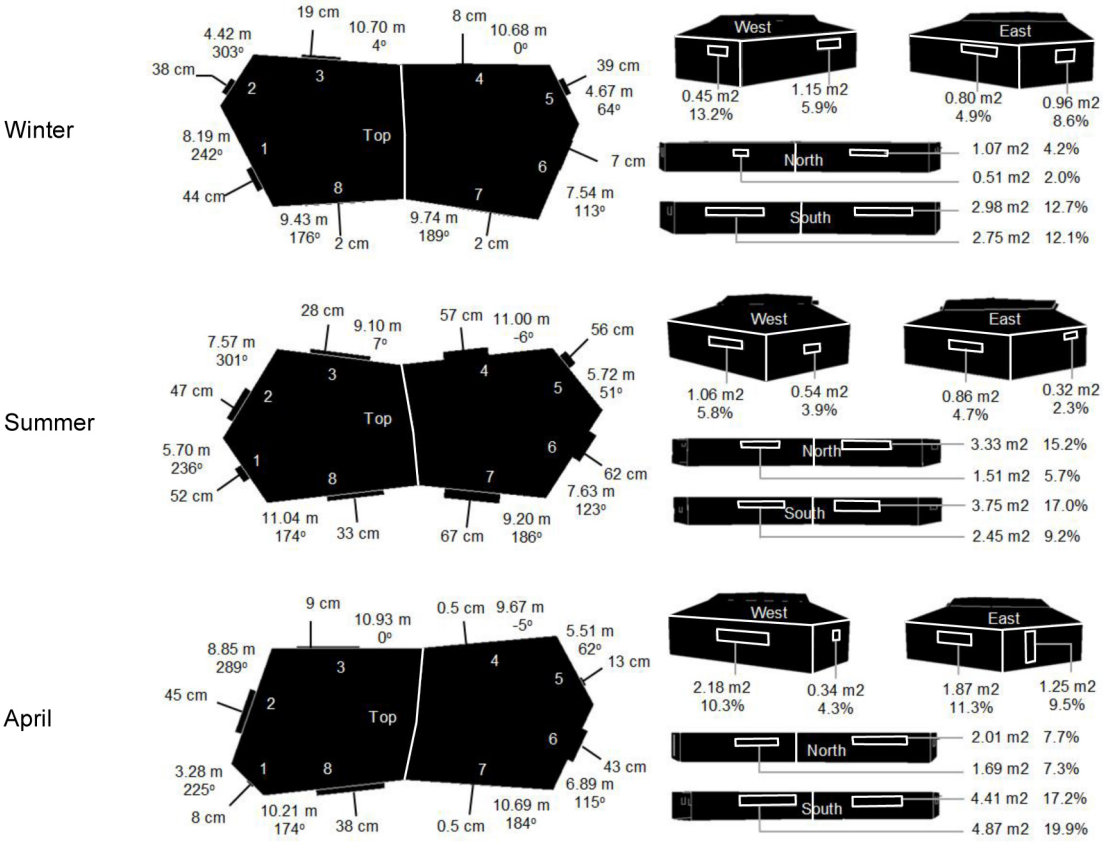

Fig. 19 Final, optimal designs found for the winter, summer and April scenarios. Note how the optimum is different for each season, yet obvious similarities of plan are found

Both winter and summer runs result in similar floor shapes. The solar azimuth in January ranges from 117^o to 242^o (from north), which is consistent with the orientations of walls 1 and 6 of the winter design. This can be explained as an attempt by the system to access more sunlight. Walls 1, 2, 5 and 6 of the summer design deviate more from due east and west allowing both orientations to receive more hours of solar radiation during which the lower solar altitude makes overhang shading less effective.

The runs in April evolved more diverse floor shapes, which implies that when energy consumption is not dominated by one driving force, variation of the less significant parameters will not cause large changes in energy performance, making for more design alternatives with equal performance.

4.3 Occupancy density scenarios

The optimised designs of the alternative occupancy scenarios are described and analysed in this section. The two levels of occupancy density are 0.2 person/m^2 (termed 0.2 occupancy) and 0.4 person/m^2 (termed 0.4 occupancy).

As seen in Fig. 20, shading depths in general increase with occupancy density. More glazing is seen on all east and west facades in the 0.4 occupancy design and the ventilation set-point drops slightly (to 20.2^{o}C). The evolved floor shapes in both runs with increased occupancy scenarios are also different from that of the 0.1 occupancy scenario presented in Fig. 19.

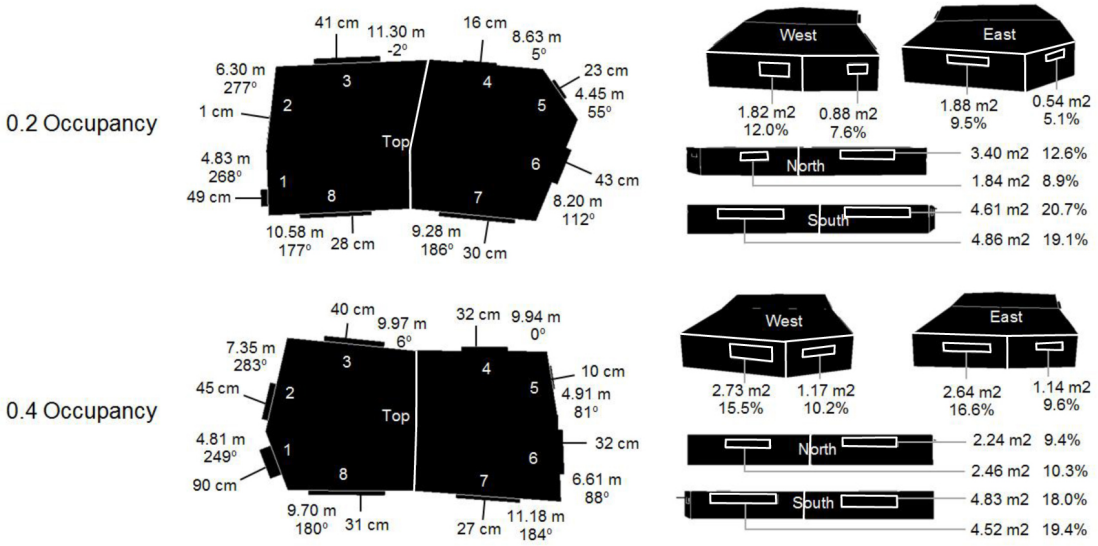

Fig. 20 Best design found for occupancies of 0.2 and 0.4 person per m^2 in April. Note the very different form for the two occupancy densities

Although the overhangs of the two designs have different depths (especially on walls 1, 2, 5 and 6), they provide similar shading, and the diversity probably arises from EnergyPlus finding difficult to show a large enough difference between them to force the evolution towards a single solution.

Heating and cooling demand are well balanced in the 0.1 occupancy scenario and the extra energy consumption when occupancy increase is basically for cooling. Comparison of the free cooling from ventilation and the mechanical cooling load profile (Fig. 21) suggests that the evolved designs under increased occupancy may sacrifice their daylight performance for better ventilation. Walls 7 and 8 are more parallel to walls 4 and 3 respectively and the axis perpendicular to the walls is closer to the prevailing wind direction. As the wind pressure coefficients are

always of opposite sign on opposite sides and reach the maximal difference at a wind incident angle of 90^o, the ventilation rate can be expected to increase with this configuration.

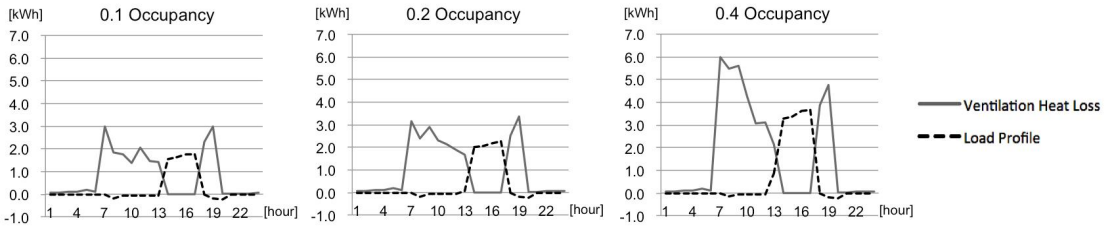

Fig. 21 Ventilation loss and cooling load profile associated with the best-fit designs in the three occupancy scenarios

4.4 Ventilation strategy scenarios

The ventilation scenarios are described and analysed in this section. In the cross ventilation (CV) scenario, only the windows on the south and north facing facades (walls 7, 8 and 3, 4) are operable, while in the mechanical ventilation (MV) scenario, ventilation is provided only by mechanical system at a constant flow at 10 L/(sperson).

As shown in Fig. 22, the area of the north facing windows and the window on wall 6 increases significantly in the best design of the CV scenario. The floor shape becomes closer to the designs found under the 0.2 occupancy scenario, and is expected to provide better ventilation. This is probably an adaptation to balance the solar gain and the ventilation loss with the changed/reduced operable windows, so the south and north facing walls need to be more parallel and the windows on walls 3 and 4 enlarged. This leads to less protrusive east and west facades due to area compensation. Simulation of the same building configuration as the CV design with all windows open (and the same set-point) shows continuous heating demand before 13:00 and after 19:00, namely the CV design could only balance the heating and cooling with the east and west windows closed. Thus it can be seen that even changes in the distribution of operable and fixed windows can lead to different preference in facade orientations for a naturally ventilated building.

The MV design shows similar features as the summer design, including deep shading on most walls, and smaller windows on the fairly protrusive east and west facades; however the windows on the north facing walls are much bigger. This is probably due to much less solar radiation being received from the north. Cooling

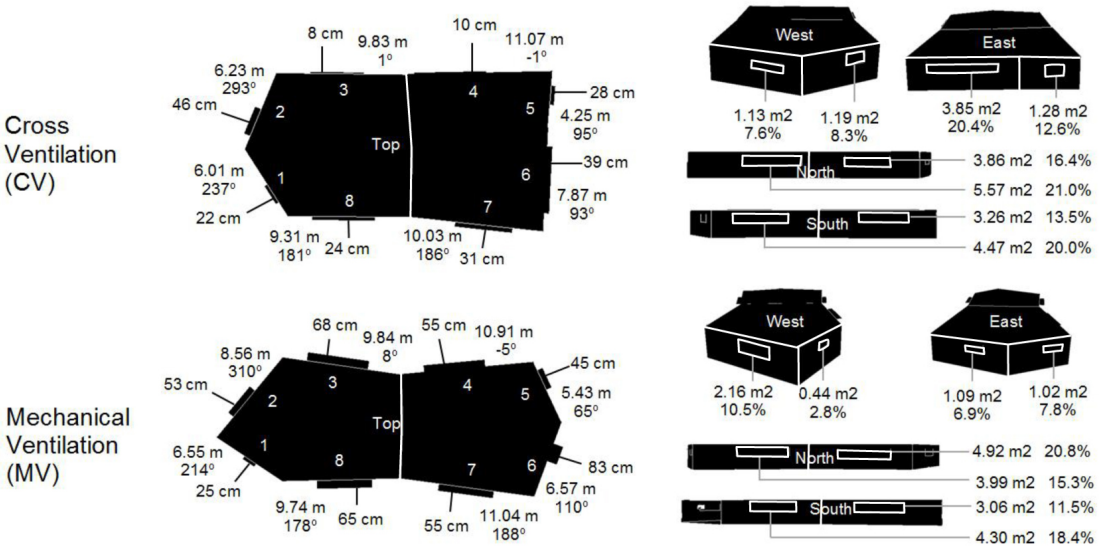

Fig. 22 Best-fit design in cross ventilation (CV) and mechanical ventilation (MV) scenarios in April

accounts for nearly all the increase in energy use. Ventilation is turned on all the time and the constant flow rate (10 L/(sperson)) is not sufficient to remove the excessive heat and keep the rooms below the cooling set-point (Fig. 23). The system needs to provide a variable flow rate with the peak at 80 L/(sperson) to neutralise the excessive gains and therefore maintain the comfort levelsclearly this is impossible. The reduction of cooling load thus relies on mitigating solar gains, which could explain the increase in shading depth and walls 1, 2 and 5, 6 being rotated away from due west and east.

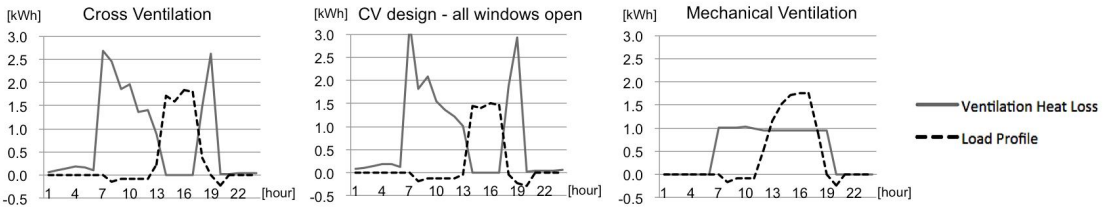

Fig. 23 Ventilation loss and load profile associated with the best designs in the ventilation strategy scenarios

4.5 Full-year optimisation

We performed a full-year optimisation to verify the ability of the methodology to produce design solutions with minimised operational energy consumption over a year. This run applies the same parameters as used for the seasonal scenarios, and the solution is obtained after an optimisation run of 30 hours.

As shown in Fig. 24, the best design solution for the full-year optimisation displays the following features in comparison with the best designs of the seasonal scenarios. (1) The overall distribution of glazing (window area and glazing ratio) is relatively close to that of the summer design. (2) The depth of shading overhang on the south, west and east facing facades is also similar between the two designs. (3) However, the shading on the north facade is small (compared with those seen on the runs for winter). (4) The orientation of the south and north facing walls are similar to those found in the summer runs. (5) However, walls 1, 2, 5, and 6 are deviate less from true west and east.

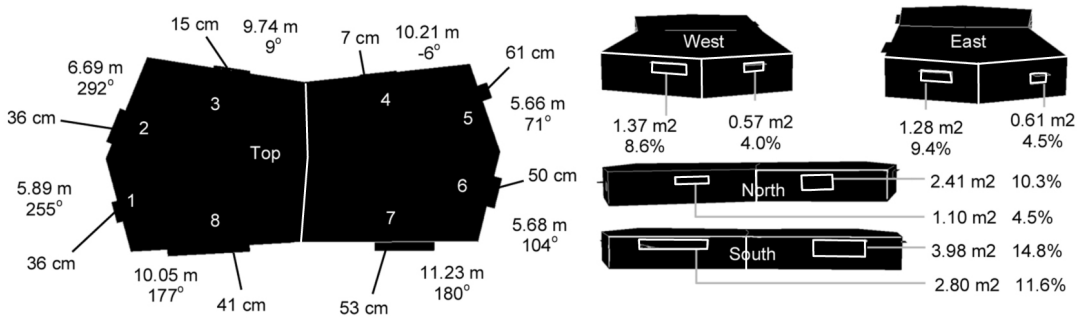

Fig. 24 Best design solution produced by the full-year optimisation

The annual total energy demand of this annual design solution is 55.97 kWh/m^2, and its monthly energy consumption is listed in Table 6 alongside the best designs of the seasonal scenarios. It can be seen that the design is competitive with all three seasonal best designs, demonstrating the ability of the methodology in searching for design solution with an optimal annual energy performance.

Table 6 Monthly energy consumption of the best design under full-year optimisation compared with the best seasonal designs

Month	Jan	Feb	Mar	Apr	May	Jun	Jul	Aug	Sep	Oct	Nov	Dec
Full-year run (kWh/m^2)	2.86	2.32	2.62	2.49	4.94	5.92	10.33	10.49	5.67	2.76	2.98	2.58
seasonal run (kWh/m^2)	2.86	–	–	2.19	–	–	–	9.22	–	–	–	–

5 Summary and conclusions

In this work a tool for the optimisation of complex multifacetted facades has been developed and proven effective. The tool was written with the aim of minimising energy consumption in multi-zoned buildings, but could be used for any other objective function, for example build cost. The tool is based on linking a GA to EnergyPlus using an effective encoding of geometry. This required a series of novel approaches needing to be developed to ensure designs would survive crossover and mutation and still form complete, buildable forms. The unique elements of the approach are: node-based floor description/encoding associated with a relative origin (to minimise isomorphism and epistasis), external node categorisation according to connection to internal nodes coupled with an area compensation scheme (to minimise inter-zone conflicts due to the evolution/variation of facets).

The final suite of programs was applied to a two-zone building design with eight facets (the tool is capable of handling up to twenty facets). Multiple runs under winter and summer scenarios for Hangzhou in China produced a series of low energy designs, with repeated architectural characteristics and hence a clear topology of form can be extracted. Runs for April, when the overall energy consumption is not dominated by either just cooling or heating, present a far greater diversity. This is a very interesting result, and underlines the view that human judgment can still be useful even within an optimising framework. Over the simulation the total annual energy consumption was found to drop from 120 kWh/m^2 to 55.97 kWh/m^2. This value is considerably lower than the typical energy demand for heating, cooling, ventilation and lighting for offices (115 kWh/m^2) in this part of China (Xie et al. 2007).

A rapid convergence of glazing ratio is observed in all runs, and the converged configurations are distinct between different scenarios of occupancy density, ventilation strategy etc., indicating their significance in energy performance despite the complexity of the facade. The optimal location of windows is almost always within the top-half of the wall regardless of the scenarios, presumably to encourage good lighting and thereby reduce energy use (this is in agreement with the optimisation work of Wright and Mourshed (2009)).

The size of the optimal shading system is seen to rapidly grow during the evolution process, particularly for mechanically cooled designs. The rate of convergence of the length and orientation of the walls during the evolution is much slower, or even non-existent, indicating a high degree of flexibility without significant change in the performance of the design: this is an extremely important architectural result, and again points to the importance of human-based interpretation of optimisation result if implementing the methodology in design.

The optimisation performed in this paper is implicitly multi-objective (i.e. minimising heating, cooling and artificial lighting energy), yet we have treated it as single-objective. However, there is no foreseeable technical barrier that would stop future users of the methodology implementing it as a multi-objective optimisation problem using a ranking scheme designed for multi-objective optimisation problems; for instance, Pareto optimality (Deb 2001).

References

AIA (2011). Defining the Architects Basic Services. Available at http://www.aia.org/aiaucmp/groups/ek_members/documents/pdf/aiap026834.pdf. Accessed 20 Apr 2012.

Bouchlaghem N (2000). Optimising the design of building envelopes for thermal performance. *Automation in Construction*, 10: 101-112.

Caldas GL, Norford KL (2002). A design optimisation tool based on a genetic algorithm. *Automation in Construction*, 11: 173-184.

Chouchoulas O (2003). Shape evolution: An algorithmic method for conceptual architectural design combining shape grammars and genetic algorithms. PhD Thesis, University of Bath, UK.

Chronis A, Turner A, Tsigkari M (2011). Generative fluid dynamics: Integration of fast fluid dynamics and genetic algorithms for wind loading optimisation of a free form surface. In: Proceedings of 2011 Symposium on Simulation for Architecture and Urban Design, Boston, USA.

Coley DA, Winters D (1997). Genetic algorithm search efficacy in aesthetic product spaces. *Complexity*, 3: 23-27.

Coley DA (1999). An Introduction to Genetic Algorithm for Scientists and Engineers. Singapore: World Scientific Publishing.

Coley DA, Schukat S (2002). Low-energy design: Combining computer-based optimisation and human judgement. *Building and Environment*, 37: 1241-1247.

Crawley DB, Lawrie LK, Winkelmann FC, Buhl WF, Huang YJ, Pedersen CO, Strand RK, Liesen RJ, Fisher DE, Witte MJ, Glazer J (2001). EnergyPlus: Creating a new-generation building energy simulation program. *Energy and Buildings*, 33: 319-331.

Deb K (2001). Multi-Objective Optimization Using Evolutionary Algorithms. Chichester, UK: John Wiley & Sons.

Elezkurtaj T, Franck G (2001). Evolutionary Algorithms in Urban Planning. In: Proceedings of CORP 2001, Vienna, Austria, pp. 269-272.

Fry B, Reas C (2012). Overview: A Short Introduction to the Processing Software and Projects from the Community. Available at http://processing.org/about. Accessed 20 Apr 2012.

Gianni Botsford Architects (2005). Light House. Available at http://www.giannibotsford.com/project/light-house. Accessed 19 Apr 2012.

Goldberg DE (1989). Genetic Algorithms in Search, Optimization, and Machine Learning. Reading, UK: Addison-Wesley.

Holland J (1975). Adaptation in Natural and Artificial Systems: An Introductory Analysis with Applications to Biology, Control and Artificial Intelligence. Ann Arbor, USA: The University of Michigan Press.

Holst JN (2003). Using whole building simulation models and optimizing procedures to optimise building envelope design with respect to energy consumption and indoor environment. In: Proceedings of 8th International IBPSA Conference, Eindhoven, the Netherlands.

Kawakita G (2008). Environmental optimisation methods in sustainable design process: In combination with evolution-based digital technology. Master Thesis, Oxford Brookes University, UK.

Kohonen J (1999). A Brief Comparison of Simulated Annealing and Genetic Algorithm Approaches. Department of Computer Science, University of Helsinki, Finland.

Kolarevic B (2000). Digital morphogenesis and computational architectures. In: Proceedings of 4th SiGRaDi Conference, Rio de Janeiro, Brazil.

LBNL (2010). Input Output Reference: The Encyclopedic Reference to EnergyPlus Input and Output. Enrest Orlando Lawrence Berkely National Laboratory, USA.

Marks W (1997). Multicriteria optimisation of shape of energy-saving buildings. *Building and Environment*, 32: 331-339.

Mitchell M (1998). An Introduction to Genetic Algorithms. Cambridge, UK: The MIT Press.

Peippo K, Lund PD, Vartiainen E (1999). Multivariate optimisation of design trade-offs for solar low energy buildings. *Energy and Buildings*, 29: 189-205.

Ramallo-Gonzlez, AP, Coley DA (2014). Using self-adaptive optimisation methods to perform sequential optimisation for low-energy building design. *Energy and Buildings*, 81: 18–29.

Rosenman MA, Gero J (1999). Evolving Designs by Generating Useful Complex Gene Structures. In: Bentley P (ed), Evolutionary Design by Computers. San Francisco: Morgan Kaufman.

Schlegel A (2012). controlP5: A GUI (Graphical User Interface) Library for Processing. Available at http://www.sojamo.de/libraries/controlP5. Accessed 16 May 2012.

Stiny G, Gips J (1972). Shape grammars and the generative specification of painting and sculpture. In: Freiman VC (ed), Proceedings of IFIP Congress 71, Amsterdam: North-Holland Publishing Company.

Tuhus-Dubrow D, Krarti M (2010). Genetic-algorithm based approach to optimize building envelope design for residential buildings. *Building and Environment*, 45: 1574-1581.

Turrin M, Buelow P, Stouffs R (2011). Design explorations of performance driven geometry in architectural design using parametric modelling and genetic algorithms. *Advanced Engineering Informatics*, 25: 656-675.

U.S. Department of Energy (2012). Weather Data. Available at http://apps1.eere.energy.gov/buildings/energyplus/cfm/weather_data3.cfm/region=2_asia_wmo_region_2/country=CHN/cname=China. Accessed 8 Jun 2012.

Wang W, Rivard H, Zmeureanu, R (2006). Floor shape optimisation for green building design. *Advanced Engineering Informatics*, 20: 363-378.

Watanabe S (2000). The IIIrd Generation of THE INDUCTION CITIES/INDUCTION DESIGN: Web Frame/Program Generated Architecture. Available at http://www.makoto-architect.com/idc2000/index2.htm. Accessed 15 May 2012.

Wetter M, Wright J (2004). A comparison of deterministic and probabilistic optimisation algorithms for nonsmooth simulationbased optimisation. *Building and Environment*, 39: 989-999.

Wetter M (2005). BuildOptA new building energy simulation program that is built on smooth models. *Building and Environment*, 40: 1085-1092.

Wright J, Mourshed M (2009). Geometric optimisation of fenestration. In: Proceedings of 11th International IBPSA Conference, Glasgow, UK.

Xie D, Zhang G, Zhou J, Zhang Q (2007). Analysis of building energy efficiency strategies for the hot sumber and cold winter zone in China. In: Proceedings of 10th International IBPSA Conference, Beijing, China.

Zhou G, Ihm P, Krarti M, Liu S, Henze GP (2003). Integration of an internal optimisation module within EnergyPlus. In: Proceedings of 8th International IBPSA Conference, Eindhoven, the Netherlands.